

Bloch oscillations in lattice potentials with controlled aperiodicity

Stefan Walter [‡], Dominik Schneble and Adam C. Durst [§]

Department of Physics and Astronomy, Stony Brook University, Stony Brook, NY
11794-3800, USA

E-mail: dschneble@stonybrook.edu

Abstract. We numerically investigate the damping of Bloch oscillations in a one-dimensional lattice potential whose translational symmetry is broken in a systematic manner, either by making the potential bichromatic or by introducing scatterers at distinct lattice sites. We find that the damping strongly depends on the ratio of lattice constants in the bichromatic potential, and that even a small concentration of scatterers can lead to strong damping. Moreover, mean-field interactions are able to counteract aperiodicity-induced damping of Bloch oscillations.

PACS numbers: 03.75.-b, 67.85.Hj, 72.10.Fk

[‡] present address: Dept. of Physics, Univ. Würzburg, Germany

[§] present address: Photon Research Associates, Port Jefferson, NY

1. Introduction

The oscillatory motion of particles in a periodic potential, when subject to an external force, was predicted by Felix Bloch in 1928 [1]. Bloch oscillations were first observed in the 1990s both in semiconductor superlattices [2], and in systems of laser-cooled atoms in optical lattices [3, 4]. Since then, they have also been studied in atomic quantum gases [5, 6, 7, 8], and have found applications in ultracold-atomic physics based precision measurements [9, 10, 11, 12].

Bloch oscillations are absent in solids due to fast damping from scattering by defects and phonons. Their observation in long-period semiconductor superlattices relies on oscillation periods that are shorter than the characteristic scattering lifetime, and even in those systems, damping of Bloch oscillations due to disorder is ubiquitous [13, 14]. In contrast, such damping is absent in optical lattice systems which are inherently defect-free, allowing for the observation of a large number of oscillations [6, 7, 8]. Damping can however be induced by the introduction of disorder into the lattice potential, which can in principle be done with various techniques [15, 16, 17, 18, 19]. Also, in the case of quantum gases, a damping of Bloch oscillations arises from mean-field interactions between weakly interacting, Bose-condensed atoms [20, 21, 22, 23, 24, 7, 8]. In the presence of both interactions and disorder, a reduction of disorder-induced damping due to screening of disorder by the mean field has been predicted [25]. Experiments with ultracold atoms thus not only constitute a versatile testbed for behavior expected in solid-state systems, but they may also display novel effects.

Recently, the damping of Bloch oscillations in a Bose-Einstein condensate [26] has been observed for an optical lattice with a superimposed randomly corrugated optical field. A related theoretical investigation of disorder-induced damping of Bloch oscillations has considered the case of Gaussian spatial noise [25]. In this paper, we numerically investigate the dynamics of an atomic wavepacket in a potential with a systematically degraded translational symmetry, considering two scenarios: the first is based on the use of a weak bichromatic potential [16] of a variable wavelength ratio, and the second considers scatterers (impurities) pinned at single sites of the potential [17]. We find that the damping strongly depends on the ratio of lattice constants in the bichromatic case, and that even a small concentration of scatterers can lead to strong damping. We also include effects of the mean-field interaction, and find that the rate at which damping of the Bloch oscillations occurs is reduced, similar to the case of Gaussian disorder [25]. Both effects should be observable experimentally with existing ultracold-atom technology.

This paper is organized as follows: After a brief discussion of fundamental aspects of tilted lattices in Sec. 2, Sec. 3 investigates the influence of aperiodicity on the damping dynamics of Bloch oscillations. Sec. 4 addresses the interplay of aperiodicity and the interaction between atoms. Conclusions are given in Sec. 5.

2. Tilted periodic potentials

The Hamiltonian for the motion of a particle in a one-dimensional periodic potential $V(x) = V(x + a)$ with lattice constant a possesses a complete set of eigenfunctions that obey Bloch's theorem $\varphi(x + a) = e^{ika}\varphi(x)$. The corresponding eigenvalues $E_n(k)$ are periodic in momentum space and form energy bands, $E_n(k + K) = E_n(k)$ (where n is the band index, $\hbar k$ the quasimomentum, and $K = 2\pi/a$ the width of the first Brillouin zone). Under the influence of an externally applied constant force ("tilt") F , the quasimomentum evolves as $\hbar k(t) = \hbar k_0 + Ft$. Due to the periodicity of the energy bands, this results in oscillations of the particle's group velocity $v_{g,n}(k) = (1/\hbar) dE_n(k)/dk$. These oscillations occur with a period $T_B = 2\pi/\omega_B = h/(aF)$ and a maximum displacement $2A_{B,n} = \Delta_n/F$ in coordinate space, where $\Delta_n = |E_n(K/2) - E_n(0)|$ is the width of the n -th band.

In the following, we consider particles that are confined to the lowest Bloch band, $n=1$, corresponding to sufficiently deep potentials and small enough tilts such that Zener tunneling [27] at the band edges is negligible. Using the split-operator method [28], we perform numerical simulations of the dynamics of Bloch oscillations of a Gaussian wave packet

$$\psi(x, t = 0) = \frac{1}{(2\pi\sigma^2)^{1/4}} \exp\left[-\frac{x^2}{(2\sigma)^2}\right] \quad (1)$$

that evolves according to the Hamiltonian

$$H = -\frac{\hbar^2 \partial_x^2}{2m} + V_0 \cos(Kx) + \tilde{V}(x) + Fx \quad (2)$$

for motion in a tilted periodic potential $V(x) = V_0 \cos(Kx) + Fx$ that is modified by a weak additional potential $\tilde{V}(x)$.

3. Effects of modified periodicity

This section investigates the influence of the additional potential $\tilde{V}(x)$, which either is a weak additional periodic potential with variable lattice constant, or arises from the local interaction with scatterers pinned at single sites of the tilted periodic potential. In the absence of $\tilde{V}(x)$, the energies of neighboring sites differ by a fixed amount $Fa = \hbar\omega_B$, corresponding to a spatially homogeneous phase difference $\Delta\phi(t) = \omega_B t$. In the presence of $\tilde{V}(x)$, $\Delta\phi$ generally becomes position-dependent, leading to global dephasing and thus to a broadening of the wave packet in momentum space, as illustrated in Fig. 1.

3.1. Bichromatic potentials

A tunable bichromatic potential is generated by the addition of

$$\tilde{V}(x) = \gamma V_0 \cos(\alpha Kx), \quad (3)$$

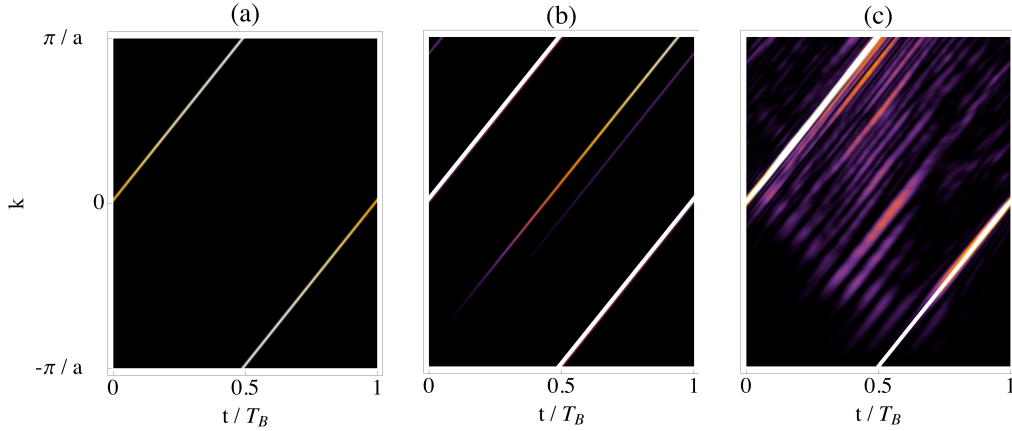


Figure 1. Evolution of the momentum-space density $|\psi(k, t)|^2$ (a) in a tilted periodic potential (b) in the presence of an additional periodic potential, and (c) in the presence of two localized scatterers as discussed in the text. Additional momentum components emerge in (b) and (c), broadening the momentum distribution. The parameters in (b) are $\gamma = 0.01$ and $\alpha = 1/\sqrt{5}$; the scatterers in (c) are spaced 11 sites apart.

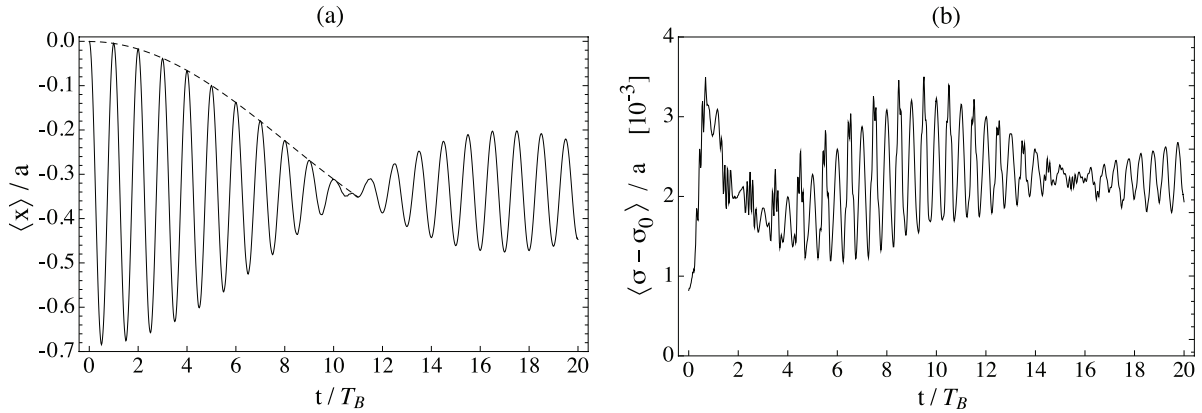


Figure 2. Damped Bloch oscillations in a bichromatic lattice ($\gamma = 0.005$, $\alpha = 0.4$). The collapse of the oscillations in coordinate space (a) is accompanied by breathing-mode excitations of the wave packet (b), and vice versa. The dashed line in (a) is the envelope $A \exp(-\eta t^2) + B$.

with variable relative amplitude $\gamma \ll 1$ and lattice-constant ratio α . If α is a rational number $\alpha = p/q$, the total potential has a periodicity $\Lambda = aq$. If furthermore Λ exceeds the spatial range probed by the wave packet, the potential can be considered disordered.

The evolution of the wave packet (Eq. 1) typically exhibits collapses and revivals of center-of-mass oscillations that are coupled to breathing-mode excitations, as is shown in Fig. 2. To characterize the decay of Bloch oscillations, the numerical data for their initial decay, for a given γ and α , are fitted with the function

$$f(t) = A \exp(-\eta t^2) \cos(\omega_B t) + B. \quad (4)$$

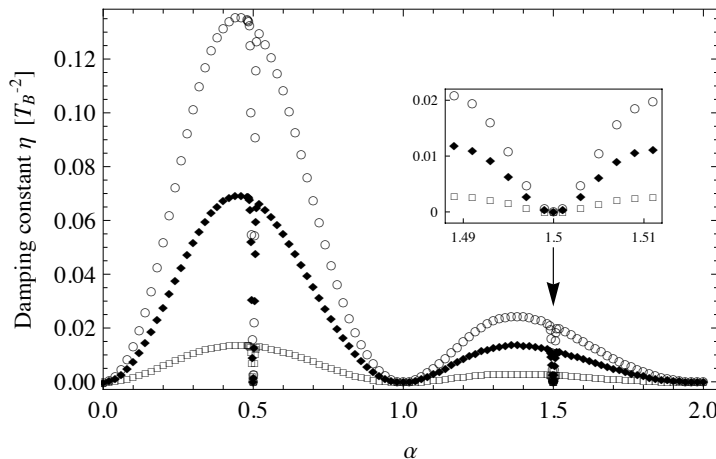


Figure 3. Damping constant η as a function of the lattice-constant ratio α , for three different depth ratios: $\gamma = 0.005$ (squares), $\gamma = 0.01$ (diamonds) and $\gamma = 0.013$ (circles). The inset shows the behavior of the decay constant in the vicinity of $\alpha = 1.5$.

Results for the Gaussian-decay constant η are shown in Fig. 3.

Clearly an increase in the perturbation amplitude γ leads to an overall increase in the damping of the oscillations. However, the dependence of the damping on the ratio α is less trivial. For integer values of α , the potential retains its original periodicity and no dephasing of Bloch oscillations occurs. It is also suppressed for half-integer values of α (i.e. for $q = 2$), which correspond to a doubling of the lattice constant, and correspondingly a halving of the Brillouin zone, and of the corresponding Bloch period. For this case, the dynamics of the wave packet in the modified band structure can easily be visualized. The shape of the band is essentially that of $V(x)$, but it is folded back into the new Brillouin zone, thus forming a closed loop, with a small splitting $\tilde{\Delta} \propto \gamma$ at the new zone boundaries (cf. Fig. 4). In one Bloch cycle, most of the wave function tunnels through the tiny gap from the lower to the upper portion at one boundary and then back to the lower portion at the other boundary. The time needed for one such cycle is T_B , i.e. the Bloch period for the unperturbed potential $V(x)$. This behavior can directly be seen in the time dependence of the overlap of the wave function with the initial wave packet $|\langle \psi(x, 0) | \psi(x, t) \rangle|$, which has a periodicity of T_B ; contributions at odd multiples of $T_B/2$ only grow very slowly over a large number of cycles.

The dynamics of Bloch oscillations in Figs. 2 and 3 are for a wavepacket with width $\sigma_0 = 20a$ in a lattice with depth $V_0 = 10 E_r$ (where $E_r \equiv (\hbar K/2)^2/2m$ is the recoil energy), and a small external force $F = 0.011 V_0/a$. In coordinate space the amplitude of the Bloch oscillations is $A_B = 0.34 a$. The additional lattice $\tilde{V}(x)$ is chosen to have a small relative amplitude $\gamma = 0.005$, which is sufficient to cause noticeable damping already after a few Bloch cycles, depending on the lattice constant ratio α .

Experimentally, such a bichromatic potential is straightforward to realize in the context of optical lattices, using two laser beams of different wavelength. With present-day tunable-laser technology, a large fraction of the range of α shown in Fig. 3 can be

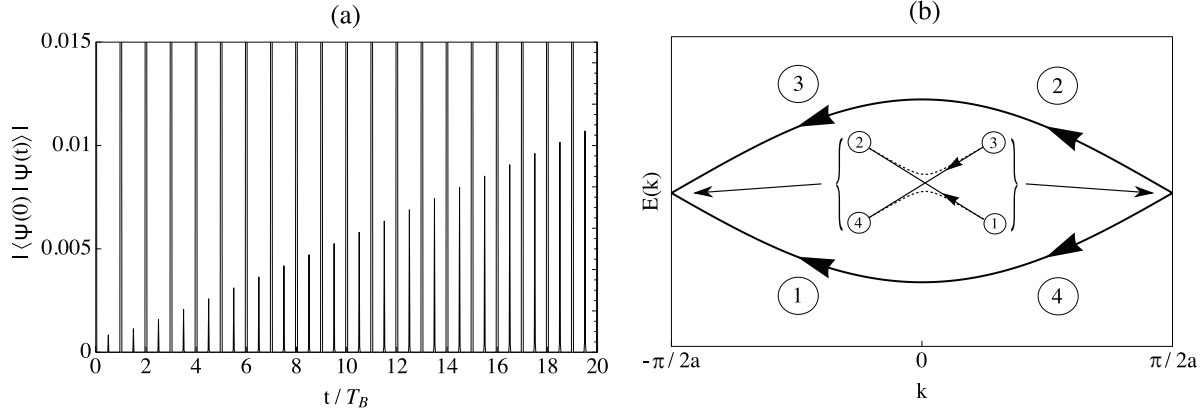


Figure 4. Wavepacket in a bichromatic potential with $\alpha = 1/2, \gamma = 0.005$. (a) Overlap $|\langle \psi(x, t=0) | \psi(x, t) \rangle|$, exhibiting the original periodicity of T_B , with small, growing, contributions at odd multiples of $T_B/2$. (b) Band structure of the potential. The inset shows the small gap at the Brillouin zone boundaries, with a calculated width $\tilde{\Delta} = 9.5 \times 10^{-5} E_r$. The arrows indicate the motion of the particle in k -space. The wave function fulfills one Bloch cycle after T_B because most of the wave function tunnels across the gap.

accessed.

3.2. Scatterers on distinct sites

For scatterers pinned at a set of distinct sites $\{n\}$ of the lattice, we model the potential \tilde{V} as a sum of Gaussians

$$\tilde{V}(x) = \sum_{\{n\}} \tilde{A} \exp \left[-(x - x_n)^2 / (2\tilde{\sigma}^2) \right]. \quad (5)$$

For the simulation, the parameters of the optical lattice and the tilt are chosen such that the size σ of the wavepacket and its oscillation amplitude A_B in the unperturbed tilted potential each cover a large number of lattice sites. A small number of scatterers are then randomly placed within the range of the wavepacket's motion. The amplitude \tilde{A} and width $\tilde{\sigma}$ of the scatterers are chosen such that the valleys of the unperturbed potential $V_0 \cos(Kx)$ are effectively filled up where the scatterers are located. Their effect on the Bloch oscillations is shown in Fig. 5. The general trend with an increasing number of scatterers is a more rapid damping of the Bloch oscillations, with the details of the dynamics depending on their spatial arrangement. Clearly, already a small number of scatterers can lead to a rapid damping of Bloch oscillations.

The results shown in Fig. 5 are for a comparatively shallow lattice ($V_0 = 1.4 E_r$) and a tilting force $F = 0.022 E_r/a$, resulting in a large amplitude $A_B = 16 a$ for undamped Bloch oscillations. The above condition for the scatterers is well fulfilled by setting $\tilde{\sigma} = \pi a/20$ and $\tilde{A} = E_r$.

In the context of ultracold atoms, the placement of scatterers pinned at single lattice sites can be achieved e.g. by using atoms with two internal states in conjunction with a state-dependent lattice depth [29], or by using two atomic species in a species-dependent optical lattice [30].

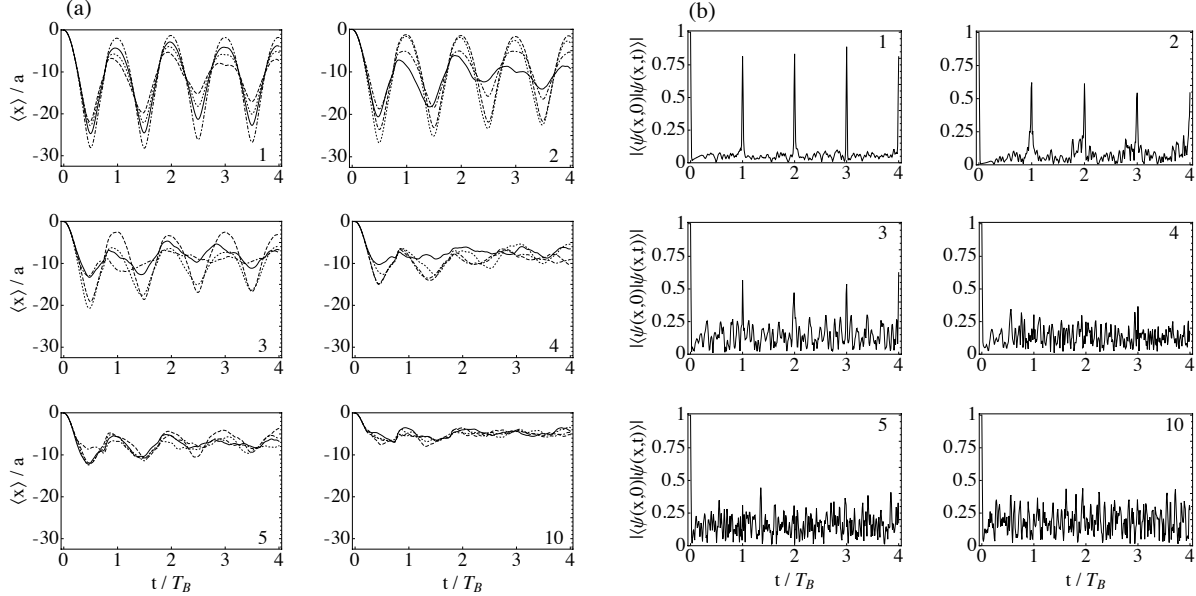


Figure 5. (a) Evolution of the packet position $\langle x(t) \rangle$ in the presence of randomly distributed scatterers. Increasing the number of scatterers (as indicated) increases the damping of Bloch oscillations. Each curve in a plot represents a different spatial configurations. (b) Overlap with the initial wave function for the case of randomly distributed scatterers. The parameters for (a) and (b) are given in the text.

4. Effect of Interactions

The discussion so far has been restricted to non-interacting particles. We now consider the case of a Bose-Einstein condensate of N atoms with repulsive interparticle interaction $U(x_i - x_j) = g\delta(x_i - x_j)$. The evolution of the condensate wavefunction $\psi(x, t) = \sqrt{N} \phi(x, t)$ in the bichromatic potential is then determined by the mean-field Hamiltonian

$$H = H_0 + \gamma V_0 \cos(\alpha K x) + gN|\phi(x, t)|^2. \quad (6)$$

The simulation results (Fig. 6) show that an increase in the coupling strength g leads to a reduction of the damping constant η , up to a characteristic value g_c , beyond which an increase in g leads to an increase in η . We interpret the reduction of η as a partial screening of the potential corrugations by the mean-field [25] as g increases, which is eventually overcompensated by mean-field induced dephasing [21, 22].

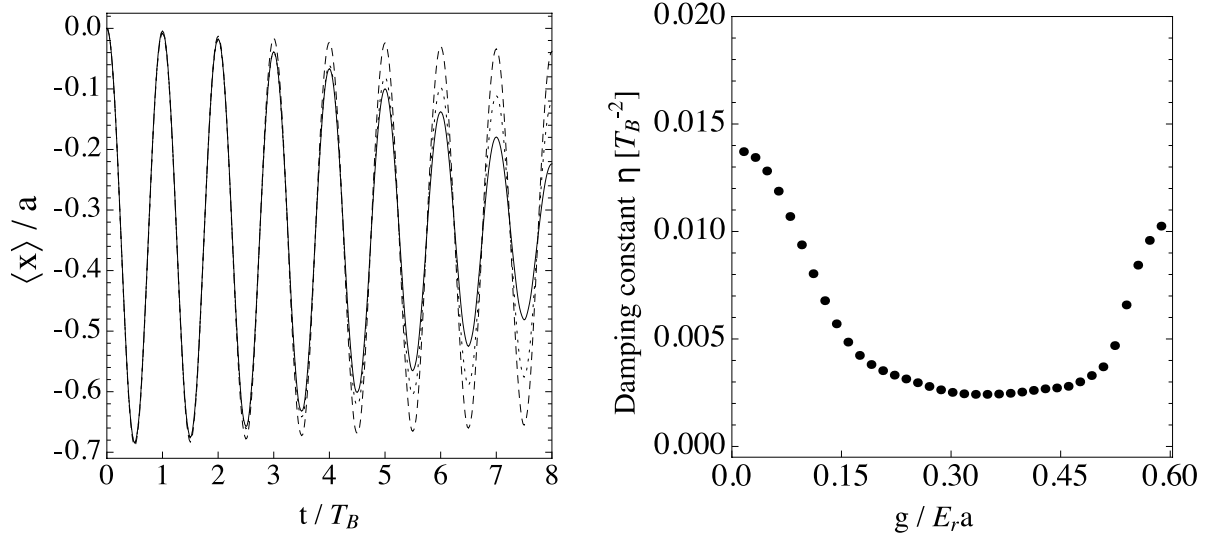


Figure 6. Interplay between aperiodicity and mean-field interaction. (a) Evolution for $g = 0$ (solid), $g = 0.1 E_r a$ (dotted), $g = 0.4 E_r a$ (dashed) (b) Dependence of η on the coupling constant g , reaching a minimum at $g_c = 0.33 E_r a$

The parameters for the simulation are the same as those in Sec. 3.1, leading to an associated coupling strength $g_c = 0.33 E_r a$. This value should be compared with an effective 1D interaction parameter $g = g_{3D}/(2\pi a_\perp^2)$ for a trapped atomic Bose-Einstein condensate, where $g_{3D} = 4\pi\hbar^2 a_s N/m$ (with atomic s-wave scattering length a_s and atomic mass m), and $a_\perp \sim R$, where R is the Thomas-Fermi radius. Already for a small condensate of ^{87}Rb atoms with $N = 1 \times 10^4$ atoms and $R = 5.3 \mu\text{m}$ in an isotropic 50 Hz trap [31], and an optical lattice with $a = 532 \text{ nm}$, we obtain $g \sim 0.42 E_r a$, which is in the vicinity of g_c . Hence, a significant modification of the damping rate in a bichromatic potential due to mean-field effects can be expected; the coupling g depends e.g. on the atom number N in the condensate which is variable. Alternatively, an investigation of the interplay is possible for species in which the mean-field interaction can be tuned via a Feshbach resonance. In this context we mention that Bloch oscillations with widely controllable mean-field interactions in a (monochromatic) optical lattice have recently been demonstrated with cesium condensates [7, 8].

5. Conclusions

We have numerically investigated the damping of Bloch oscillations resulting from a controlled breakdown of the periodicity of the lattice potential. The effects discussed here, including the effects of the mean-field interaction on disorder-induced dephasing, should be readily observable in experiments with ultracold atoms in optical lattices.

Acknowledgments

We thank D. Pertot and B. Gadway for a critical reading of the manuscript. This work is supported by NSF Grants No. DMR-0605919 (S.W. and A.C.D) and PHY-0855643 (D.S.) as well as a DAAD scholarship (S.W.).

References

- [1] F. Bloch. *Z. Phys.*, 52:555, 1928.
- [2] C. Waschke, H.G. Roskos, R. Schwedler, K. Leo, H. Kurz, and K. Köhler. *Phys. Rev. Lett.*, 70:3319, 1993.
- [3] S. R. Wilkinson, C. F. Bharucha, K. W. Madison, Qian Niu, and M. G. Raizen. *Phys. Rev. Lett.*, 76:4512, 1996.
- [4] Maxime Ben Dahan, Ekkehard Peik, Jakob Reichel, Yvan Castin, and Christophe Salomon. *Phys. Rev. Lett.*, 76:4508, 1996.
- [5] O. Morsch, J. H. Müller, M. Cristiani, D. Ciampini, and E. Arimondo. *Phys. Rev. Lett.*, 87:140402, 2001.
- [6] G. Roati, E. de Mirandes, F. Ferlaino, H. Ott, G. Modugno, and M. Inguscio. *Phys. Rev. Lett.*, 92:230402, 2004.
- [7] M. Gustavsson, E. Haller, M. J. Mark, J. G. Danzl, G. Rojas-Kopeinig, and H.-C. Nägerl. *Phys. Rev. Lett.*, 100:080404, 2008.
- [8] M. Fattori, C. D’Errico, G. Roati, M. Zaccanti, M. Jona-Lasinio, M. Modugno, M. Inguscio, and G. Modugno. *Phys. Rev. Lett.*, 100:080405, 2008.
- [9] Rémy Battesti, Pierre Cladé, Saïda Guellati-Khélifa, Catherine Schwob, Benoît Grémaud, François Nez, Lucile Julien, and François Biraben. *Phys. Rev. Lett.*, 92:253001, 2004.
- [10] I. Carusotto, L. Pitaevskii, S. Stringari, G. Modugno, and M. Inguscio. *Phys. Rev. Lett.*, 95:093202, 2005.
- [11] G. Ferrari, N. Poli, F. Sorrentino, and G. M. Tino. *Phys. Rev. Lett.*, 97:060402, 2006.
- [12] Pierre Cladé, Estefania de Mirandes, Malo Cadoret, Saïda Guellati-Khélifa, Catherine Schwob, François Nez, Lucile Julien, and François Biraben. *Phys. Rev. Lett.*, 96:033001, 2006.
- [13] G. von Plessen, T. Meier, J. Feldmann, E. O. Göbel, P. Thomas, K. W. Goossen, J. M. Kuo, and R. F. Kopf. *Phys. Rev. B*, 49:14058, 1994.
- [14] E. Diez, F. Domínguez-Adame, and A. Sánchez. *Microelectron. Eng.*, 43-44:117, 1998.
- [15] Peter Horak, Jean-Yves Courtois, and Gilbert Grynberg. *Phys. Rev. A*, 58:3953, 1998.
- [16] Roberto B. Diener, Georgios A. Georgakis, Jianxin Zhong, Mark Raizen, and Qian Niu. *Phys. Rev. A*, 64:033416, 2001.
- [17] Uri Gavish and Yvan Castin. *Phys. Rev. Lett.*, 95:020401, 2005.
- [18] S. Ospelkaus, C. Ospelkaus, O. Wille, M. Succo, P. Ernst, K. Sengstock, and K. Bongs. *Phys. Rev. Lett.*, 96:180403, 2006.
- [19] Daw-Wei Wang, Mikhail D. Lukin, and Eugene Demler. *Phys. Rev. Lett.*, 92:076802, 2004.
- [20] Biao Wu and Qian Niu. *Phys. Rev. A*, 64:061603, 2001.
- [21] M. Holthaus. *J. Opt. B: Quantum Semiclassical Opt.*, 2:589, 2000.
- [22] D. Witthaut, M. Werder, S. Mossmann, and H.J. Korsch. *Phys. Rev. E*, 71:036625, 2005.
- [23] C Menotti, A Smerzi, and A Trombettoni. *New J. Phys.*, 5:112, 2003.
- [24] M. Modugno, C. Tozzo, and F. Dalfovo. *Phys. Rev. A*, 70:043625, 2004.
- [25] T. Schulte, S. Drenkelforth, G. Kleine Büning, W. Ertmer, J. Arlt, M. Lewenstein, and L. Santos. *Phys. Rev. A*, 77:023610, 2008.
- [26] S Drenkelforth, G Kleine Büning, J Will, T Schulte, N Murray, W Ertmer, L Santos, and J J Arlt. *New J. Phys.*, 10:045027, 2008.
- [27] C. Zener. *Proc. R. Soc. Lond. A*, 145:523, 1934.

- [28] M. D. Feit, J. A. Fleck Jr., and A. Steiger. *J. Comput. Phys.*, 47:412, 1982.
- [29] B. Gadway et al. in preparation, 2009.
- [30] J. Catani, G. Barontini, G. Lamporesi, F. Rabatti, G. Thalhammer, F. Minardi, S. Stringari, and M. Inguscio. *Phys. Rev. Lett.*, 103:140401, 2009.
- [31] D. Pertot, D. Greif, S. Albert, B. Gadway, and D. Schneble. *J. Phys. B: At. Mol. Opt. Phys.*, 42:215305, 2009.